

1 Mercury Sorption and Desorption on Organo-Mineral Particulates as 2 a Source for Microbial Methylation

3 Lijie Zhang,^{†,¶} Shan Wu,^{†,‡,¶} Linduo Zhao,^{†,¶} Xia Lu,^{†,¶} Eric M. Pierce,^{†,¶} and Baohua Gu*,^{†,§,¶}

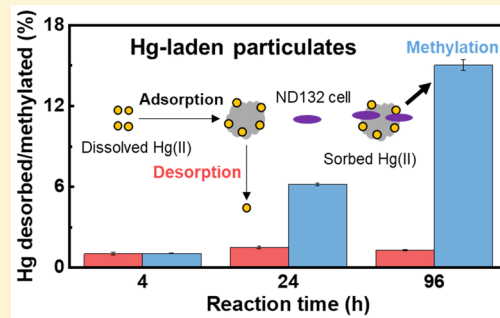
4 [†]Environmental Sciences Division, Oak Ridge National Laboratory, Oak Ridge, Tennessee 37831, United States

5 [‡]School of Resource, Environmental and Chemical Engineering, Nanchang University, Nanchang 330031, China

6 [§]Department of Biosystems Engineering and Soil Science, University of Tennessee, Knoxville, Tennessee 37996, United States

7 Supporting Information

ABSTRACT: In natural freshwater and sediments, mercuric mercury (Hg(II)) is largely associated with particulate minerals and organics, but it remains unclear under what conditions particulates may become a sink or a source for Hg(II) and whether the particulate-bound Hg(II) is bioavailable for microbial uptake and methylation. In this study, we investigated Hg(II) sorption–desorption characteristics on three organo-coated hematite particulates and a Hg-contaminated natural sediment and evaluated the potential of particulate-bound Hg(II) for microbial methylation. Mercury rapidly sorbed onto particulates, especially the cysteine-coated hematite and sediment, with little desorption observed (0.1–4%). However, the presence of Hg-binding ligands, such as low-molecular-weight thiols and humic acids, resulted in up to 60% of Hg(II) desorption from the Hg-laden hematite particulates but <6% from the sediment. Importantly, the particulate-bound Hg(II) was bioavailable for uptake and methylation by a sulfate-reducing bacterium *Desulfovibrio desulfuricans* ND132 under anaerobic incubations, and the methylation rate was 4–10 times higher than the desorption rate of Hg(II). These observations suggest direct contacts and interactions between bacterial cells and the particulate-bound Hg(II), resulting in rapid exchange or uptake of Hg(II) by the bacteria. The results highlight the importance of Hg(II) partitioning at particulate–water interfaces and the role of particulates as a significant source of Hg(II) for methylation in the environment.



26 ■ INTRODUCTION

27 Mercury (Hg) is a global pollutant and can be methylated to
28 form methylmercury (MeHg), a neurotoxin, which can
29 bioaccumulate and biomagnify in food webs.^{1,2} Certain
30 microorganisms, such as sulfate-reducing bacteria,^{3,4} iron-
31 reducing bacteria,^{5,6} and methanogens,^{7–9} contain a two-gene
32 cluster, *hgcAB*, responsible for converting inorganic mercuric
33 Hg(II) to MeHg.¹⁰ However, microbial methylation requires
34 the initial step of Hg(II) cellular uptake from the extracellular
35 environment,^{11–13} and the physicochemical forms of Hg in the
36 environment are known to affect its availability for uptake.^{14–18}
37 These different physicochemical forms of inorganic Hg present
38 in natural waters and sediments include, but are not limited to,
39 elemental Hg (Hg(0)), water-soluble Hg(II), mineral-bound
40 Hg(II), dissolved and particulate organic matter (DOM and
41 POM) bound Hg(II), and mercuric sulfide phases (cinnabar
42 and metacinnabar).^{14–17,19–21} In particular, minerals, DOM-
43 coated minerals (or organo-minerals), and POM are
44 ubiquitous, and up to 95% of the Hg(II) in fresh water and
45 sediments are usually associated with these solids.^{14,15,22–24}

46 Particulates may act as a sink for Hg(II) through sorption
47 and occlusion or as a source by slowly and continuously
48 releasing Hg(II) to solution for microbial uptake and
49 methylation. However, under what geochemical conditions
50 do these particulates become a sink or a source for Hg(II)

51 remains unclear in complex environmental systems, where
52 concurrent interactions may occur between Hg(II) and
53 minerals, DOM or POM, microbes, and various dissolved
54 ligands. Hg(II) is known to strongly sorb onto soil organic
55 matter, minerals, and biomass,^{11,14–17,23,25} although its
56 mobility and bioavailability on particulates depend on the
57 surrounding environment, such as the presence or absence of
58 various Hg-binding ligands in solution. For example, low-
59 molecular-weight (LMW) thiols are common in living
60 organisms and often found in extracellular environments with
61 concentrations ranging from nM to μ M.^{26–29} These thiol
62 compounds have high affinities for Hg(II) binding and in
63 particular, thiol functional groups on natural POM and DOM
64 have been shown to form exceptionally strong complexes with
65 Hg(II).^{30–33} Therefore, Hg(II) binding with these environ-
66 mentally relevant organic ligands may release and remobilize
67 particulate-bound Hg(II), making it available for microbial
68 methylation. Since minerals are often coated with DOM or
69 POM, Hg(II) sorption and desorption behavior on these
70 minerals could also be influenced by the coated organics or

Received: October 25, 2018

Revised: January 17, 2019

Accepted: January 31, 2019

Published: January 31, 2019

71 their exposed active functional groups. Previous studies
72 suggested that aqueous Hg(II) species were more bioavailable
73 than those bound to DOM or POM,^{14,23} and particulate HgS
74 was the least bioavailable form due to its extremely low
75 solubility.^{14,15,34–36} However, to date, systematic evaluations of
76 particulate-bound Hg(II) for microbial uptake and methylation
77 are lacking, especially concerning Hg(II) bound to organic
78 matter or thiol-coated minerals and natural sediments. An
79 improved understanding of the roles of complex organo-
80 mineral particulates as a sink or source for Hg(II) sorption,
81 desorption, and methylation under environmentally relevant
82 conditions is needed to predict MeHg production in the
83 environment.

84 The overall goal of this study was therefore to determine
85 Hg(II) sorption and desorption behavior at the particulate–
86 water interface and the bioavailability of particulate-bound
87 Hg(II) for microbial methylation. Specifically, using the
88 synthesized thiol- and DOM-coated hematite particulates and
89 a Hg-contaminated natural sediment, we investigated the
90 sorption/desorption kinetics and dynamics of Hg(II) and
91 evaluated the potential availability of particulate-bound Hg(II)
92 for microbial uptake and methylation by a known methylator,
93 *Desulfovibrio desulfurans* ND132, in laboratory cultures.

94 ■ EXPERIMENTAL SECTION

95 **Chemicals.** Cysteine, glutathione, and sodium 2,3-dimer-
96 capto-1-propanesulfonate monohydrate (DMPS) were used as
97 LMW thiols. Elliott soil humic acids (HA) was obtained from
98 the International Humic Substances Society (IHSS), contain-
99 ing 58.13% C (w/w) and 0.44% S (w/w). An EFPC-DOM was
100 isolated from East Fork Poplar Creek (EFPC) water in Oak
101 Ridge, Tennessee, as previously described,³⁷ and contained
102 54.77% C (w/w) and 1.93% S (w/w). A Hg-contaminated
103 natural sediment, containing ~2% iron oxides,^{38,39} and a pure
104 hematite mineral, as commonly observed in natural soil and
105 aquatic environments, were selected for comparative studies.
106 Hematite was purchased from Stern Chemicals (Newbury-
107 port, MA) and used as received. The sediment sample was
108 collected from EFPC, oven-dried at 45 °C until a constant
109 weight, ground, screened with a 250-mesh sieve (63 µm
110 openings), and then stored in a desiccator in the dark until use.
111 The sediment contained about 16.1 µg/g total Hg, 10 mg/g C,
112 and 0.2 mg/g S.

113 **Mercury Adsorption Experiments.** Four particulate
114 samples were used to investigate Hg(II) adsorption and
115 include pure hematite, cysteine-coated hematite, EFPC-DOM-
116 coated hematite, and a Hg-contaminated EFPC-sediment. The
117 organic matter-coated hematite was prepared by reacting
118 hematite (5 g/L) with either cysteine (10 mM) or EFPC-
119 DOM (0.24 g/L) in 1 mM NaCl solution in amber glass vials.
120 The suspensions were shaken for 24 h and vacuum filtered
121 through 0.45 µm membrane filters (Millipore). The organic-
122 coated hematite was then washed three times with 1 mM NaCl
123 (5 mL each), scraped off the filters, and oven-dried at 45 °C
124 until a constant weight was obtained. Adsorption isotherms of
125 Hg(II) were subsequently determined on these particulates
126 with a solid concentration of 0.1 g/L in 1 mL NaCl at pH 6.5
127 in sealed glass vials under ambient conditions. An aliquot of
128 the Hg(II) stock solution was added to a series of amber glass
129 vials to obtain an initial Hg(II) concentration of 1 to 50 µg/L.
130 Samples were then equilibrated on a rotary shaker for 24 h,
131 which was found to be sufficient to reach an adsorption
132 equilibrium based on initial kinetic studies. For detailed kinetic

133 studies, the initial Hg(II) concentration was fixed at 10 µg/L,
134 and samples were taken and analyzed at desired time intervals
135 of 1, 2, 4, 12, 24, and 48 h. For Hg(II) analysis, duplicate
136 sample vials were sacrificed, and samples were filtered through
137 0.2 µm syringe filters. The filtrate was preserved in 5% (v/v)
138 BrCl solution (in 0.2 M HCl) overnight or longer at 4 °C, and
139 an aliquot was used for determining Hg(II) concentration via
140 reduction with SnCl₂ to purgeable Hg(0) and detection using a
141 Lumex RA-915+ analyzer (Ohio Lumex Co., Cleveland, OH).
142 The detection limit of the method was about 10 pg Hg.^{11,37,40}
143 The amount of Hg(II) adsorbed was calculated by the
144 difference between the initial Hg(II) concentration and the
145 amount measured in the filtrate solution. Data points in all
146 figures represent an average of 4–6 replicate samples (at least
147 duplicate batch experiments), and error bars represent the
148 standard deviations.

149 **Mercury Desorption Experiments.** Hg(II) desorption
150 from Hg-laden minerals and the EFPC-sediment was
151 subsequently investigated in the presence of various organic
152 ligands (HA and thiols). The Hg-contaminated EFPC-
153 sediment was used without further treatment. The Hg-laden
154 hematite, cysteine-coated hematite, and EFPC-DOM-coated
155 hematite were prepared in laboratory by reacting Hg(II) (0.5
156 mg/L, 20 mL) with 0.2 g hematite, cysteine-coated, and DOM-
157 coated-hematite, respectively, in 1 mM NaCl solution at pH
158 6.5 in sealed amber glass vials. Samples were then equilibrated
159 for 24 h on a rotary shaker and vacuum filtered through 0.45
160 µm membrane filters. The particulates were again washed with
161 1 mM NaCl and oven-dried before use.

162 Desorption kinetics of Hg(II) was studied similarly with the
163 DOM-coated hematite (1 g/L) and the EFPC-sediment (5 g/
164 L). A higher sediment concentration was used because of its
165 relatively low desorption. HA (8 mg C/L) or DMPS (100 µM)
166 was added to the suspension, and the vials were shaken for
167 desired time intervals (1, 2, 4, 8, 24, 72, and 120 h) for Hg(II)
168 desorption. Similarly, Hg(II) desorption from Hg-laden
169 particulates was also conducted in the presence of different
170 concentrations of HA (0–40 mg C/L) and thiols (cysteine,
171 glutathione, and DMPS at 0–200 µM) in 1 mM NaCl at pH
172 6.5. Samples were equilibrated for 24 h and then filtered and
173 analyzed, as described in the sorption experiment.

174 **Mercury Methylation Assays with Hg-Laden Partic-
175 ules.** The bioavailability of the particulate-bound Hg(II)
176 was assayed by the production of MeHg by a known
177 methylator, *Desulfovibrio desulfurans* ND132, under anaerobic
178 conditions. The *D. desulfurans* ND132 strain was cultured,
179 harvested, and washed using previously established proto-
180 cols.^{11,37,41} A series of 1 g/L Hg-laden cysteine-coated
181 hematite and 2 g/L EFPC-sediment suspensions were
182 prepared in deoxygenated phosphate-buffered saline (PBS),
183 consisting of 0.14 M NaCl, 3 mM KCl, 10 mM Na₂HPO₄, and
184 2 mM KH₂PO₄ at pH 7.4. The washed ND132 cells were
185 added to the suspension to a final cell density of 10⁸ cells/mL
186 and then supplemented with 1 mM pyruvate and 1 mM
187 fumarate as the respective electron donor and acceptor. All
188 vials were immediately sealed with PTFE-lined silicone screw
189 caps and shaken in the anaerobic chamber in the dark. Control
190 experiments were conducted similarly with particulates in PBS
191 but without cells. At desired time intervals, replicate sample
192 vials were collected and preserved in HCl (0.5% v/v) at 4 °C
193 until analysis. An aliquot (0.05–0.2 mL) was used for total
194 MeHg analysis with a modified EPA Method 1630, as
195 previously described.^{10,11,37,40,41} The detection limit for
196

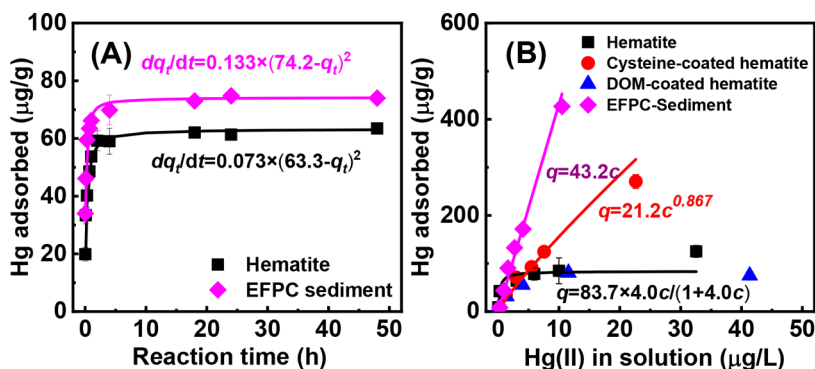


Figure 1. (A) Hg(II) sorption kinetics (at the initial Hg concentration of 10 μg/L) and (B) sorption isotherms on 0.1 g/L hematite and EFPC-sediment suspended in 1 mM NaCl solution at pH 6.5. Solid lines are fitted curves using linear (EFPC-sediment), Freundlich (cysteine-coated hematite), and Langmuir (hematite) model equations noted in the figure.

196 MeHg was ~6 pg/L Hg. The remaining aliquot was oxidized
 197 with BrCl (5% v/v) overnight and analyzed for total Hg using
 198 a Lumex RA-915+ analyzer. Control samples (without cells)
 199 were filtered through 0.2 μm syringe filters, and the filtrates
 200 were analyzed for total Hg(II) in the same manner.

RESULTS AND DISCUSSION

Mercury Adsorption on Organo-Hematite Particulates and EFPC Sediment. Sorption kinetics of Hg(II) were evaluated first on hematite and the EFPC-sediment (Figure 1A). In both cases, the sorption increased rapidly within the first 2 h, and the rate decreased and reached equilibrium in ~4 h. The kinetics appeared to follow a pseudo-second-order reaction with estimated rate constants of 0.073 and 0.133 g μg⁻¹ h⁻¹ on hematite and the EFPC-sediment, respectively (Supporting Information, Figure S1). The amount of Hg(II) adsorbed at equilibrium was 63.3 μg/g on hematite and 74.2 μg/g on the EFPC-sediment at the initial Hg(II) concentration of 10 μg/L and the particulate concentration of 0.1 g/L.

Hg(II) sorption isotherms were subsequently determined using hematite, cysteine-coated hematite, EFPC-DOM-coated hematite, and the EFPC-sediment (Figure 1B and Table S1), representing various organo-mineral particulates found in the natural environment. Hematite and the EFPC-DOM-coated hematite exhibited similar sorption behavior for Hg(II): the sorption first increased with increasing aqueous Hg(II) concentrations and reached a maximum sorption capacity of ~84 μg/g on both hematite and the EFPC-DOM-coated hematite. However, Hg(II) sorption on cysteine-coated hematite increased much more than that on the bare hematite or the DOM-coated hematite and did not show a maximum within the Hg(II) concentration ranges studied (up to 50 μg/L). The EFPC-sediment showed the highest affinity and capacity for Hg(II) sorption among all the particulates studied (Figure 1B).

The observed differences in Hg(II) sorption affinity and capacity on particulates (Figure 1) could be explained by different mineral surface characteristics and binding sites for Hg(II). Iron oxide adsorbs DOM through surface complexation-ligand exchange reactions with the carboxyl and hydroxyl functional groups on DOM.^{42,43} The amount of DOM adsorbed on hematite was estimated to be ~1.5 mg C/g hematite (0.15 mg C/L) at pH 6.5 in 0.1 M NaCl, based on previous studies (Figure S2).^{42,43} As a conservative estimate, if we assume that 50% of the sulfur (total 1.93%) on EFPC-DOM is reduced and the strong binding sites (−SH) represent

2% of the reduced sulfur,^{31,44} the total binding sites on the EFPC-DOM adsorbed on hematite would be ~3.5 nmol/g hematite. This small amount of −SH on EFPC-DOM-coated hematite thus did not induce observable differences in Hg(II) sorption from the bare hematite. However, a much higher amount of cysteine was adsorbed on hematite at neutral pH (up to 26 mg/g, or ~0.2 mmol/g thiols on the surface) (S2),⁴⁵ although partial oxidation of cysteine is expected under ambient conditions.^{45,46} A substantially higher amount of Hg(II) adsorbed by the cysteine-coated hematite than the bare hematite and the DOM-coated hematite (Figure 1B) suggests that the adsorbed cysteine remained effective in binding with Hg(II). For the EFPC-sediment, it exhibited the highest sorption capacity for Hg(II) (Figure 1B), although the sediment already retained a substantial amount of Hg(II) (Table S2). This high sorption capacity by the EFPC-sediment may be explained not only by surface adsorption but also immobilization by a heterogeneous mixture of various POM, biomass, and minerals in the sediment,^{30,31,47} which contained about 10 mg/g C and 0.2 mg/g S. Soil organic matter and biomass, such as microbial cells and periphyton, are known to adsorb or rapidly take up Hg(II) from aqueous solution.^{37,40,48–50} Taking into account the low sorption capacity of hematite and the DOM-coated hematite, it is reasonable to assume that the presence of organic matter and biomass in the EFPC-sediment are likely responsible for its higher Hg(II) sorption capacity.

Mercury Desorption from Hg-Laden Hematite Particulates and EFPC-Sediments. Hg(II) desorption kinetics from the Hg-laden DOM-coated hematite and the EFPC-sediment was investigated in the presence of either 100 μM DMPS or 8 mg C/L HA (Figure 2). The initial loading of Hg(II) on the DOM-coated hematite was 14.6 μg/g, which was ~20 times higher than the estimated thiols on the adsorbed DOM, suggesting that other functional groups on DOM (e.g., carboxyl and amine) or direct binding with hematite were also involved in Hg(II) adsorption. The EFPC-sediment was used without further treatment, with an initial Hg(II) loading of 16.1 μg/g (Table S2). Hg(II) desorption by DMPS proceeded rapidly within the first 24 h and reached a plateau between 24 and 120 h for both the DOM-coated hematite and the EFPC-sediment. However, a smaller fraction of Hg(II) was desorbed from the EFPC-sediment (0.72 μg/g, or <5% of the total Hg) than that from the DOM-coated hematite (~7.5 μg/g, or ~50%). Interestingly, Hg(II) desorption by HA was much lower than that by DMPS,

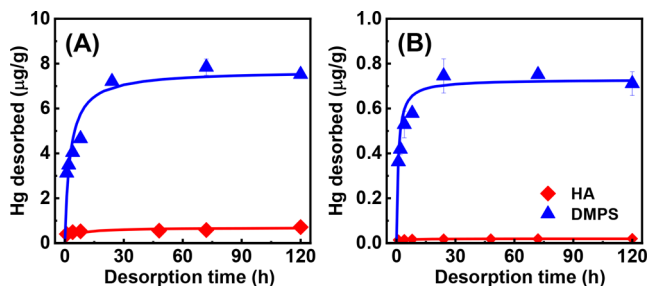


Figure 2. Hg(II) desorption kinetics from (A) Hg-laden EFPC-DOM-coated hematite (1 g/L) and (B) EFPC-sediment (5 g/L) with 8 mg C/L HA or 100 μ M DMPS at pH 6.5 in 1 mM NaCl. Solid lines are fitted curves based on rate equations in Table S3.

although HA or DOM is also known to form strong complexes with Hg(II).^{26,30,33} The amount of Hg(II) desorbed by HA was <4% and <0.15% from the Hg-laden DOM-coated hematite and the EFPC-sediment, respectively (Figure 2). The ineffectiveness of HA in desorbing Hg(II) was attributed to a lower amount of $-SH$ functional groups on HA than on DMPS. It was estimated that the HA contained a reactive $-SH$ concentration in the range of 21–310 nM at 8 mg C/L,^{31,51} which is much lower than the added DMPS (100 μ M, or 200 μ M $-SH$). However, when normalized to the available concentrations of $-SH$ functional groups, the ability of $-SH$ in HA in desorbing Hg(II) was in fact comparable to that of DMPS, consistent with strong binding affinities of Hg(II) with both HA and DMPS.^{30,52}

To further investigate Hg(II) desorption or mobilization, different concentrations of HA and LMW thiols (i.e., DMPS, cysteine, and glutathione) were used in Hg(II) desorption from three Hg-laden hematite particulates and the EFPC-sediment (Table S2). Without addition of HA or thiols, Hg(II) desorption upon wetting of the particles was generally low, ranging from 0.1 to 4% of the initially loaded Hg(II) (Figure 3). Desorption was higher from Hg-laden DOM-coated hematite (~4%) than from Hg-laden cysteine-coated hematite (~0.5%) and from Hg-laden hematite (~0.1%) (Figure 3), likely due to the desorption of some weakly bound Hg(II) or Hg-DOM or Hg-thiol complexes upon wetting. As expected, addition of HA or thiols resulted in substantially increased Hg(II) desorption due to strong competitive binding of HA and thiols for the adsorbed Hg(II), although the amount of desorption varied greatly with the type and concentrations of HA or thiols and the Hg-laden particulates themselves. Hg(II) desorption by HA from the three Hg-laden organo-hematite was relatively low but increased with increasing HA concentrations (Figure 3, left column). Hg(II) desorption by the LMW thiols (Figure 3, right column) was 4–40 fold higher than that by HA, resulting from the addition of a higher amount of available $-SH$ functional groups. With the addition of 50 μ M LMW thiols, Hg(II) desorption increased to ~20% from the Hg-laden hematite, and further increasing thiol concentrations (up to 200 μ M) desorbed only a slightly higher amount of Hg(II). This trend of Hg(II) desorption by LMW thiols was similar on all three Hg-laden organo-hematite particulates. The ability of DMPS, cysteine, and glutathione in desorbing Hg(II) was comparable, with the exception of Hg(II) desorption by cysteine from the Hg-laden cysteine-coated hematite. In this case, a significantly lower amount of Hg(II) (~10%) was desorbed by cysteine than by glutathione or DMPS (~60%) since Hg(II) was already bound to cysteine

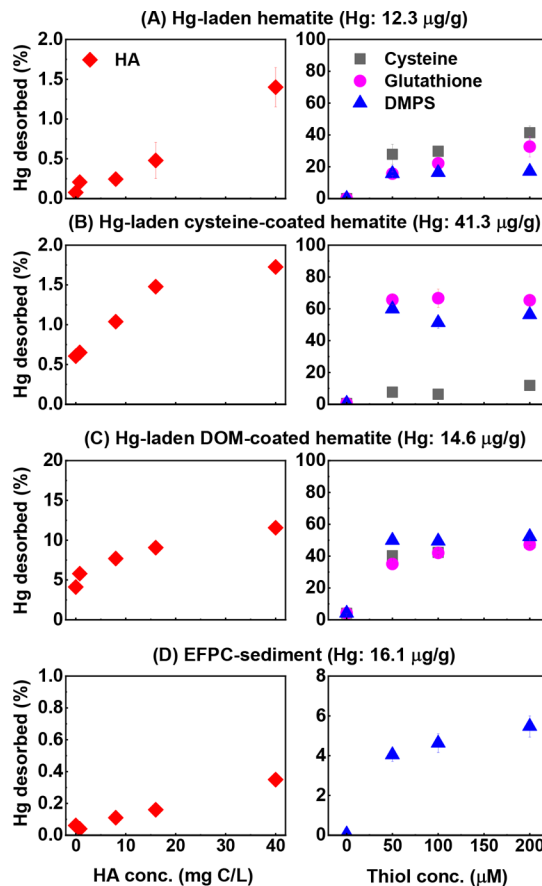


Figure 3. Hg(II) desorption from (A) Hg-laden hematite, (B) Hg-laden cysteine-coated hematite, (C) Hg-laden DOM-coated hematite, and (D) EFPC-sediment with varying concentrations of HA or LMW thiols (cysteine, glutathione, and DMPS) in 1 mM NaCl at pH 6.5 for 24 h. The added particulate concentration was 1 g/L for Hg-laden hematite and 5 g/L for the EFPC-sediment.

on the hematite surface. The result also implies that the adsorbed Hg(II)-cysteine on hematite was stable, but glutathione and DMPS were able to outcompete cysteine for Hg(II) desorption.

Interestingly, we observed a higher amount of Hg(II) desorption from the DOM-coated hematite (40–55%) or cysteine-coated hematite (50–70%) than the Hg-laden hematite (20–40%). This observation was surprising because Hg(II) bound to hematite surfaces was thought to be more readily desorbed by thiols than from the thiol-bound Hg(II) on the DOM- or cysteine-coated hematite, as Hg(II) would be strongly bound to the $-SH$ functional groups.^{23,30,33,51} The lower Hg(II) desorption from the Hg-laden hematite than from the Hg-laden cysteine-coated hematite suggests that Hg(II) was likely sorbed or immobilized more strongly on hematite, making it more resistant to desorption. Previous EXAFS studies proposed the formation of an inner-sphere complex between Hg(II) and goethite via two oxygen atoms bound to the Fe sites⁵³ and the potential formation of montroydite (HgO) during Hg(II) adsorption on montmorillonite and vermiculite.⁵⁴ Other studies speculated that Hg(II) can migrate and be incorporated into mineral solid matrix or diffuse into pores of minerals, making it unavailable for desorption.^{36,55,56} These immobilization mechanisms of Hg(II) likely occur on hematite as well and may thus partially explain why lower amounts of Hg(II) were desorbed from the

361 bare hematite than from the cysteine-coated hematite. 362 Alternatively, the desorbed Hg(II) (or Hg-thiol complexes) 363 could be readSORBED on hematite directly or by forming ternary 364 complexes of hematite-thiol-Hg(II), as previously de- 365 scribed.^{23,57} Hg(II) readSORPTION would compete with its 366 desorption, thereby resulting in an apparently low amount of 367 Hg(II) desorption by increasing concentrations of thiols 368 (Figure 3, right column). Similarly, for the Hg-laden DOM- 369 coated hematite, a portion of the Hg(II) could be bound 370 directly on hematite because of limited thiol-binding sites on 371 DOM. Therefore, the amount of Hg(II) desorbed from the 372 Hg-laden DOM-coated hematite was lower than that from the 373 cysteine-coated hematite but higher than that from the bare 374 hematite.

375 Of particular interest is the observation of a much lower 376 amount of Hg(II) desorbed from the EFPC-sediment than that 377 from the organo-hematite particulates by both HA and DMPS 378 (Figure 3D). Less than 0.4% and 6% of the Hg(II) on EFPC- 379 sediments was desorbed by HA and DMPS, respectively. We 380 hypothesize three possible mechanisms as to why a low 381 amount of Hg(II) desorption was observed from the EFPC- 382 sediment. First, in complex natural sediments, Hg(II) not only 383 binds with soil minerals (e.g., Fe/Mn oxides) and organic 384 matter but also forms mineral precipitates such as meta- 385 cinnabar (HgS) or nanoparticulate HgS.^{14,17,39,58} The 386 predominant forms of Hg in the EFPC-sediment were 387 characterized to be metacinnabar and organic matter-bound 388 Hg(II), with a small fraction of the Hg(II) present as the 389 sorbed Hg(II) on Fe/Mn oxides.^{17,39} We thus consider that 390 HA and DMPS could desorb Hg(II) by competing with soil 391 organic matter on the EFPC-sediment, as in the Hg-laden 392 cysteine- or DOM-coated hematite. HA and DMPS could also 393 enhance the dissolution of HgS or nanoparticulate HgS by 394 forming Hg(II)-thiol complexes,^{52,59} although previous studies 395 have shown that HgS is quite resistant to desorption and 396 dissolution by HA and thiols.^{14,17} These results support our 397 observation that lower amounts of Hg(II) could be desorbed 398 from EFPC-sediment than from the Hg-laden organo-hematite 399 particulates, where Hg(II) was bound to the surface-coated 400 organics. The fact that Hg(II) desorption or dissolution 401 increased with increasing HA or DMPS concentrations (Figure 402 3D) also suggests that Hg(II) on the EFPC-sediment was 403 more resistant to desorption than that on the Hg-laden organo- 404 hematite particulates. The second mechanism could be due to 405 the incorporation or uptake of Hg(II) to biomass in the EFPC- 406 sediment, as described earlier, making the Hg(II) less 407 accessible for desorption or dissolution. Biomass such as 408 microbial cells and phytoplankton is known to rapidly take up 409 and internalize a large portion of Hg(II).^{11,37,40,48-50} Once 410 inside the cell, Hg(II) cannot be desorbed unless cells are 411 lysed. Third, aging effects could be another factor contributing 412 to the low desorption of Hg(II) from the EFPC-sediment due 413 to potential phase transformations, changes in bonding 414 environments, and migration of Hg(II) into stable soil and 415 organic matrixes over time. Several studies have reported that 416 fresh Hg(II) loadings to waters and sediments are more 417 bioavailable and accessible than the previously deposited 418 Hg(II),^{14,36,60} consistent with our observations of lower Hg(II) 419 desorption from EFPC-sediment (with a long deposition time) 420 than from Hg-laden hematite particulates.

421 **Particulate-Bound Hg(II) as a Source for Microbial 422 Methylation.** To evaluate whether the particulate-bound 423 Hg(II) may serve as a sole source of Hg(II) for methylation,

the Hg-laden cysteine-coated hematite and the EFPC-sediment 424 were incubated directly with washed cells of *D. desulfurians* 425 ND132 in PBS, and Hg(II) desorption and methylation were 426 determined. Hg(II) desorption in the absence of ND132 cells 427 (as a control) was found to be very low in PBS (Figure 4), 428 f4

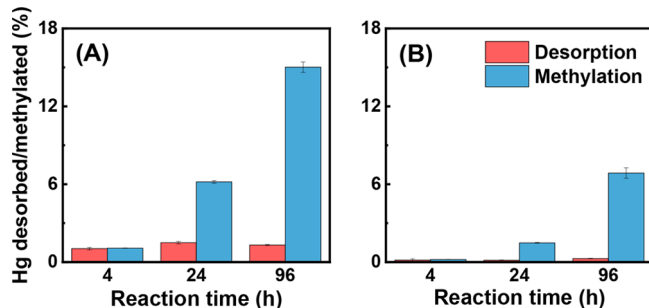


Figure 4. Hg(II) desorption (without cells) and methylation in the presence of washed cells of *D. desulfurians* ND132 (10^8 cells/mL) in PBS. (A) Hg-laden cysteine-coated hematite and (B) EFPC-sediments were used as the only Hg(II) source for Hg(II) desorption and methylation. The particulate concentration was 1 g/L for the Hg-laden cysteine-coated hematite and 2 g/L for the EFPC sediment.

similar to that observed in 1 mM NaCl solution at pH 6.5 (Figure 3). The amounts of Hg(II) desorbed were <1.5% and <0.3% after 96 h from the Hg-laden cysteine-coated hematite and the EFPC-sediment, respectively. Without ND132 cells, no MeHg production was observed in the EFPC-sediment control (data not shown), indicating negligible contributions of native microorganisms to Hg methylation in the sediment. However, a much higher amount of Hg(II) methylation was observed (Figure 4) in the presence of ND132 cells. With the Hg-laden cysteine-coated hematite, cells produced ~2.2 to 31 nM MeHg after 4–96 h reactions, equivalent to about 1–15% of the total Hg(II) on the particulates (Figure 4A). Although lower, MeHg production in EFPC-sediment by ND132 cells ranged from 0.2% to 7%, but Hg(II) desorption was negligible (<0.3%) (Figure 4B). The lower methylation observed in EFPC-sediments than in the Hg-laden cysteine-coated hematite indicates that Hg(II) in the sediment was less bioavailable, since different forms of Hg(II) and its aging time could influence the rate of Hg(II) desorption, uptake, and methylation.

Importantly, the observed higher amounts of Hg(II) methylation than desorption (Figure 4) suggest that particulate-bound Hg(II) was available for microbial uptake and methylation. This observation questions the common notion that only soluble Hg(II) (and HgS nanoparticles) are available for microbial uptake or methylation.^{14,15,61} Jonsson et al. proposed that aqueous or soluble Hg(II) was resupplied continuously by dissolution or desorption from the solids to sustain microbial methylation.^{14,15} However, we estimate that the initial Hg(II) desorption rate from Hg-laden cysteine-coated hematite (Figure 4) was only ~0.13 nM/h, much lower than the initial methylation rate of 0.53 nM/h. Similarly, the initial Hg(II) desorption rate from EFPC sediments was only ~0.01 nM/h, but the methylation rate was ~0.1 nM/h. The result cannot be attributed to the methylation of nanoparticulate HgS because of a low total Hg content observed in the filtrate solution. We hypothesize that direct contact and interactions between ND132 cells with the particulate-bound Hg(II) resulted in faster rates of Hg(II) uptake and

468 methylation, possibly through ligand exchange with thiol
469 functional groups on the cell surface rather than cell uptake of
470 the Hg(II) in the bulk solution phase.¹⁵ Abundant thiols or
471 sulfhydryl functional groups (10^6 – 10^7 thiols/cell) are known
472 to be present on ND132 cell envelopes and cytosols^{37,62} up to a
473 thiol concentration of 0.17–1.7 μM at the cell concentration of
474 10^8 cells/mL, as used in this study. While it remains unclear
475 exactly how cells take up Hg(II), cellular thiols are critically
476 important in Hg(II) acquisition and uptake.^{11,37,62,63} Another
477 possible explanation is that bacterial exudates or extracellular
478 substances may have made particulate-bound Hg(II) more
479 available for methylation. These extracellular substances may
480 include low-molecular-weight thiols or other organic ligands
481 which form complexes with Hg(II) and thus enhance Hg(II)
482 uptake and methylation.^{13,27,29} However, regardless of the
483 mechanisms, close contacts between particulate-bound Hg(II)
484 and cells could lead to continuous Hg(II) complexation and
485 exchange with the thiols on ND132 cells, resulting in
486 subsequent Hg(II) uptake and methylation (faster than the
487 rate of Hg(II) desorption without cells).

488 **Environmental Implications.** Mercury partitioning at
489 particulate–water interfaces greatly affects its fate, transport,
490 and transformation in natural water and sediments and
491 ultimately its availability for biological uptake and methyl-
492 ation.^{14,15,36} Natural sediments and organo-coated minerals,
493 such as thiol- and DOM-coated hematite commonly found in
494 soils, were all shown to have a large capacity to sorb Hg(II)
495 under suboxic environmental conditions. They may represent
496 one of the largest sinks when Hg(II) is discharged from a point
497 source^{23,47,64} or deposited from the atmosphere.^{65,66} The result
498 is consistent with the fact that most Hg(II) in soil and aquatic
499 environments is associated with solids or particulates.^{14,22–24,67}
500 However, Hg-laden particulates can also serve as a Hg(II)
501 source for biological uptake and methylation. In particular, the
502 presence of complexing organic ligands, such as small thiols,
503 can result in significant desorption of Hg(II) and facilitate its
504 release from particulates by 4–40 fold, depending on the types
505 of particulate-bound Hg(II) and the thiol content. DOM at
506 relatively low concentrations (e.g., < 5 ppm) shows a limited
507 desorption capacity, in part because of its low thiol content and
508 its competition with POM for Hg(II) binding. These
509 observations agree with studies that have shown key roles of
510 extracellular thiols in periphyton biofilms in influencing MeHg
511 production during algal bloom.^{29,68,69} Increased levels of low-
512 molecular-weight thiols could enhance microbial methylation
513 either through the formation of specific Hg(II)-thiol
514 complexes¹³ or through increased Hg(II) desorption from
515 particulates or cellular materials and thus increased bioavail-
516 ability.^{11,37} Therefore, depending on the environmental
517 conditions (e.g., minerals or organo-minerals, thiols, and
518 DOM contents), particulates may exert significant controls
519 on MeHg production in the aquatic environment.

520 Most significantly, we found that the particulate-bound
521 Hg(II) is available for microbial methylation, evidenced by the
522 higher methylation rates and extents than Hg(II) desorption
523 using Hg-laden particulates as the only Hg(II) source (Figure
524 4). This is especially evident in experiments with the sediment-
525 bound Hg(II), which resulted in >7% Hg(II) methylation but
526 <0.3% Hg(II) desorption under same experimental conditions.
527 The results signify important roles of particulates as an
528 available Hg(II) source for methylation. We propose that
529 direct contacts and interactions between particulate-bound
530 Hg(II) and cell surface thiols likely facilitated the exchange of

531 Hg(II) from particulates and consequently resulted in 531
532 increased rate of cell Hg(II) uptake and methylation. These 532
533 observations suggest an alternative pathway by which microbes 533
534 take up Hg(II) that is more complicated than we previously 534
535 thought: particulate-bound Hg(II) may not have to be 535
536 desorbed or dissolved in the aqueous phase to make it 536
537 available for microbial uptake and methylation. Microbial 537
538 methylation of particulated-bound Hg(II) should thus be 538
539 considered in predicting MeHg production in the natural 539
540 aquatic environment.
540

ASSOCIATED CONTENT

Supporting Information

The Supporting Information is available free of charge on the
ACS Publications website at DOI: [10.1021/acs.est.8b06020](https://doi.org/10.1021/acs.est.8b06020).

Hg sorption kinetics on particulates (S1), estimated
DOM and cysteine adsorption on hematite (S2), Hg
sorption isotherms on particulates (S3), Hg contents on
Hg-laden particulates (S4), Hg desorption kinetics from
Hg-laden particulates (S5) ([PDF](#))

AUTHOR INFORMATION

Corresponding Author

*Phone: (865) 574 7286. Email: gub1@ornl.gov.

ORCID

Linduo Zhao: [0000-0002-2718-4538](https://orcid.org/0000-0002-2718-4538)

Xia Lu: [0000-0003-2150-7575](https://orcid.org/0000-0003-2150-7575)

Eric M. Pierce: [0000-0002-4951-1931](https://orcid.org/0000-0002-4951-1931)

Baohua Gu: [0000-0002-7299-2956](https://orcid.org/0000-0002-7299-2956)

Author Contributions

[¶]These authors contributed equally.

Notes

The authors declare no competing financial interest.

ACKNOWLEDGMENTS

This research was sponsored by the Office of Biological and
Environmental Research within the Office of Science of the
U.S. Department of Energy (DOE), as part of the Mercury
Science Focus Area project at the Oak Ridge National
Laboratory (ORNL), which is managed by UT-Battelle, LLC
under Contract No. DE-AC05-00OR22725 with DOE. We
thank Hongmei Chen and Phuong Pham for the EFPC-DOM
isolate. S.W. was supported in part by the Chinese Scholarship
Council (CSC) of China.

REFERENCES

- Wood, J. M. Biological cycles for toxic elements in the environment. *Science* **1974**, *183* (4129), 1049–1052.
- Harris, R. C.; Rudd, J. W.; Amyot, M.; Babiarz, C. L.; Beaty, K. G.; Blanchfield, P. J.; Bodaly, R.; Branfireun, B. A.; Gilmour, C. C.; Graydon, J. A. Whole-ecosystem study shows rapid fish-mercury response to changes in mercury deposition. *Proc. Natl. Acad. Sci. U. S. A.* **2007**, *104* (42), 16586–16591.
- Compeau, G.; Bartha, R. Sulfate-reducing bacteria: principal methylators of mercury in anoxic estuarine sediment. *Appl. Environ. Microbiol.* **1985**, *50* (2), 498–502.
- Gilmour, C. C.; Henry, E. A.; Mitchell, R. Sulfate stimulation of mercury methylation in freshwater sediments. *Environ. Sci. Technol.* **1992**, *26* (11), 2281–2287.
- Fleming, E. J.; Mack, E. E.; Green, P. G.; Nelson, D. C. Mercury methylation from unexpected sources: molybdate-inhibited freshwater

588 sediments and an iron-reducing bacterium. *Appl. Environ. Microbiol.* 589 **2006**, *72* (1), 457–464.

590 (6) Kerin, E. J.; Gilmour, C. C.; Roden, E.; Suzuki, M.; Coates, J.; 591 Mason, R. Mercury methylation by dissimilatory iron-reducing 592 bacteria. *Appl. Environ. Microbiol.* **2006**, *72* (12), 7919–7921.

593 (7) Hamelin, S.; Amyot, M.; Barkay, T.; Wang, Y.; Planas, D. 594 Methanogens: principal methylators of mercury in lake periphyton. 595 *Environ. Sci. Technol.* **2011**, *45* (18), 7693–7700.

596 (8) Gilmour, C. C.; Podar, M.; Bullock, A. L.; Graham, A. M.; 597 Brown, S. D.; Somenahally, A. C.; Johs, A.; Hurt, R. A., Jr; Bailey, K. 598 L.; Elias, D. A. Mercury methylation by novel microorganisms from 599 new environments. *Environ. Sci. Technol.* **2013**, *47* (20), 11810– 600 11820.

601 (9) Yu, R.-Q.; Reinfelder, J. R.; Hines, M. E.; Barkay, T. Mercury 602 methylation by the methanogen *Methanospirillum hungatei*. *Appl. 603 Environ. Microbiol.* **2013**, *79* (20), 6325.

604 (10) Parks, J. M.; Johs, A.; Podar, M.; Bridou, R.; Hurt, R. A.; Smith, 605 S. D.; Tomanicek, S. J.; Qian, Y.; Brown, S. D.; Brandt, C. C.; 606 Palumbo, A. V.; Smith, J. C.; Wall, J. D.; Elias, D. A.; Liang, L. The 607 Genetic Basis for Bacterial Mercury Methylation. *Science* **2013**, *339* 608 (6125), 1332–1335.

609 (11) Liu, Y.-R.; Lu, X.; Zhao, L.; An, J.; He, J.-Z.; Pierce, E. M.; Johs, 610 A.; Gu, B. Effects of cellular sorption on mercury bioavailability and 611 methylmercury production by *Desulfovibrio desulfuricans* ND132. 612 *Environ. Sci. Technol.* **2016**, *50* (24), 13335–13341.

613 (12) Pedrero, Z.; Bridou, R.; Mounicou, S.; Guyoneaud, R.; 614 Monperrus, M.; Amouroux, D. Transformation, localization, and 615 biomolecular binding of Hg species at subcellular level in methylating 616 and nonmethylating sulfate-reducing bacteria. *Environ. Sci. Technol.* 617 **2012**, *46* (21), 11744–11751.

618 (13) Schaefer, J. K.; Rocks, S. S.; Zheng, W.; Liang, L.; Gu, B.; 619 Morel, F. M. Active transport, substrate specificity, and methylation of 620 Hg (II) in anaerobic bacteria. *Proc. Natl. Acad. Sci. U. S. A.* **2011**, *108* 621 (21), 8714–8719.

622 (14) Jonsson, S.; Skyllberg, U.; Nilsson, M. B.; Lundberg, E.; 623 Andersson, A.; Björn, E. Differentiated availability of geochemical 624 mercury pools controls methylmercury levels in estuarine sediment 625 and biota. *Nat. Commun.* **2014**, *5*, 4624.

626 (15) Jonsson, S.; Skyllberg, U.; Nilsson, M. B.; Westlund, P.-O.; 627 Shchukarev, A.; Lundberg, E.; Björn, E. Mercury methylation rates for 628 geochemically relevant HgII species in sediments. *Environ. Sci. 629 Technol.* **2012**, *46* (21), 11653–11659.

630 (16) Zagury, G. J.; Neculita, C. M.; Bastien, C.; Deschênes, L. 631 Mercury fractionation, bioavailability, and ecotoxicity in highly 632 contaminated soils from chlor-alkali plants. *Environ. Toxicol. Chem.* 633 **2006**, *25* (4), 1138–1147.

634 (17) Han, F. X.; Shiyan, S.; Chen, J.; Su, Y.; Monts, D. L.; Waggoner, 635 C. A.; Matta, F. B. Extractability and bioavailability of mercury from a 636 mercury sulfide contaminated soil in Oak Ridge, Tennessee, USA. 637 *Water, Air, Soil Pollut.* **2008**, *194* (1–4), 67–75.

638 (18) Schaefer, J. K.; Szczuka, A.; Morel, F. o. M. Effect of divalent 639 metals on Hg (II) uptake and methylation by bacteria. *Environ. Sci. 640 Technol.* **2014**, *48* (5), 3007–3013.

641 (19) Schartup, A. T.; Ndu, U.; Balcom, P. H.; Mason, R. P.; 642 Sunderland, E. M. Contrasting effects of marine and terrestrially 643 derived dissolved organic matter on mercury speciation and 644 bioavailability in seawater. *Environ. Sci. Technol.* **2015**, *49* (10), 645 5965–5972.

646 (20) Zhang, T.; Kim, B.; Levard, C. m.; Reinsch, B. C.; Lowry, G. V.; 647 Deshusses, M. A.; Hsu-Kim, H. Methylation of mercury by bacteria 648 exposed to dissolved, nanoparticulate, and microparticulate mercuric 649 sulfides. *Environ. Sci. Technol.* **2012**, *46* (13), 6950–6958.

650 (21) Graham, A. M.; Aiken, G. R.; Gilmour, C. C. Dissolved organic 651 matter enhances microbial mercury methylation under sulfidic 652 conditions. *Environ. Sci. Technol.* **2012**, *46* (5), 2715–2723.

653 (22) Brooks, S. C.; Southworth, G. R. History of mercury use and 654 environmental contamination at the Oak Ridge Y-12 Plant. *Environ. 655 Pollut.* **2011**, *159* (1), 219–228.

656 (23) Gu, B.; Mishra, B.; Miller, C.; Wang, W.; Lai, B.; Brooks, S. C.; 657 Kemner, K. M.; Liang, L. X-ray fluorescence mapping of mercury on 658 suspended mineral particles and diatoms in a contaminated freshwater 659 system. *Biogeosciences* **2014**, *11* (18), 5259–5267.

660 (24) Morel, F. M.; Kraepiel, A. M.; Amyot, M. The chemical cycle 661 and bioaccumulation of mercury. *Annu. Rev. Ecol. Syst.* **1998**, *29* (1), 661 543–566.

662 (25) Dunham-Cheatham, S.; Mishra, B.; Myneni, S.; Fein, J. B. The 663 effect of natural organic matter on the adsorption of mercury to 664 bacterial cells. *Geochim. Cosmochim. Acta* **2015**, *150*, 1–10.

663 (26) Skyllberg, U. Competition among thiols and inorganic sulfides 666 and polysulfides for Hg and MeHg in wetland soils and sediments 667 under suboxic conditions: Illumination of controversies and 668 implications for MeHg net production. *J. Geophys. Res. Biogeosci.* **2008**, *113*, 1–14.

669 (27) Zhang, J.; Wang, F.; House, J. D.; Page, B. Thiols in wetland 671 interstitial waters and their role in mercury and methylmercury 672 speciation. *Limnol. Oceanogr.* **2004**, *49* (6), 2276–2286.

673 (28) Oram, P. D.; Fang, X.; Fernando, Q.; Letkeman, P.; Letkeman, 674 D. The formation constants of mercury (II)–glutathione complexes. *675 Chem. Res. Toxicol.* **1996**, *9* (4), 709–712.

676 (29) Leclerc, M.; Planas, D.; Amyot, M. Relationship between 677 extracellular low-molecular-weight thiols and mercury species in 678 natural lake periphytic biofilms. *Environ. Sci. Technol.* **2015**, *49* (13), 679 7709–7716.

680 (30) Dong, W.; Bian, Y.; Liang, L.; Gu, B. Binding Constants of 681 Mercury and Dissolved Organic Matter Determined by a Modified 682 Ion Exchange Technique. *Environ. Sci. Technol.* **2011**, *45* (8), 3576– 683 3583.

684 (31) Dong, W.; Liang, L.; Brooks, S.; Southworth, G.; Gu, B. Roles 685 of dissolved organic matter in the speciation of mercury and 686 methylmercury in a contaminated ecosystem in Oak Ridge, 687 Tennessee. *Environ. Chem.* **2010**, *7* (1), 94–102.

688 (32) Liem-Nguyen, V.; Skyllberg, U.; Nam, K.; Björn, E. 689 Thermodynamic stability of mercury (II) complexes formed with 690 environmentally relevant low-molecular-mass thiols studied by 691 competing ligand exchange and density functional theory. *Environ. 692 Chem.* **2017**, *14* (4), 243–253.

693 (33) Song, Y.; Jiang, T.; Liem-Nguyen, V.; Sparrman, T.; Björn, E.; 694 Skyllberg, U. Thermodynamics of Hg(II) Bonding to Thiol Groups in 695 Suwannee River Natural Organic Matter Resolved by Competitive 696 Ligand Exchange, Hg LIII-Edge EXAFS and 1H NMR Spectroscopy. *697 Environ. Sci. Technol.* **2018**, *52* (15), 8292–8301.

698 (34) Hsu-Kim, H.; Kucharzyk, K. H.; Zhang, T.; Deshusses, M. A. 699 Mechanisms regulating mercury bioavailability for methylating 700 microorganisms in the aquatic environment: a critical review. *Environ. 701 Sci. Technol.* **2013**, *47* (6), 2441–2456.

702 (35) Zhang, T.; Kucharzyk, K. H.; Kim, B.; Deshusses, M. A.; Hsu- 703 Kim, H. Net methylation of mercury in estuarine sediment 704 microcosms amended with dissolved, nanoparticulate, and micro- 705 particulate mercuric sulfides. *Environ. Sci. Technol.* **2014**, *48* (16), 706 9133–9141.

707 (36) Hintelmann, H.; Keppel-Jones, K.; Evans, R. D. Constants of 708 mercury methylation and demethylation rates in sediments and 709 comparison of tracer and ambient mercury availability. *Environ. 710 Toxicol. Chem.* **2000**, *19* (9), 2204–2211.

711 (37) Zhao, L.; Chen, H.; Lu, X.; Lin, H.; Christensen, G. A.; Pierce, 712 E. M.; Gu, B. Contrasting Effects of Dissolved Organic Matter on 713 Mercury Methylation by *Geobacter sulfurreducens* PCA and 714 *Desulfovibrio desulfuricans* ND132. *Environ. Sci. Technol.* **2017**, *51* 715 (18), 10468–10475.

716 (38) Han, F. X.; Su, Y.; Monts, D. L.; Waggoner, C. A.; Plodinec, M. 717 J. Binding, distribution, and plant uptake of mercury in a soil from 718 Oak Ridge, Tennessee, USA. *Sci. Total Environ.* **2006**, *368* (2–3), 719 753–768.

720 (39) Liu, G.; Cabrera, J.; Allen, M.; Cai, Y. Mercury characterization 721 in a soil sample collected nearby the DOE Oak Ridge Reservation 722 utilizing sequential extraction and thermal desorption method. *Sci. 723 Total Environ.* **2006**, *369* (1–3), 384–392.

725 (40) Lu, X.; Johs, A.; Zhao, L.; Wang, L.; Pierce, E. M.; Gu, B.
726 Nanomolar Copper Enhances Mercury Methylation by Desulfovibrio
727 desulfuricans ND132. *Environ. Sci. Technol. Lett.* **2018**, *5* (5), 372–
728 376.

729 (41) Hu, H.; Lin, H.; Zheng, W.; Tomanicek, S. J.; Johs, A.; Feng,
730 X.; Elias, D. A.; Liang, L.; Gu, B. Oxidation and methylation of
731 dissolved elemental mercury by anaerobic bacteria. *Nat. Geosci.* **2013**,
732 *6* (9), 751.

733 (42) Gu, B.; Schmitt, J.; Chen, Z.; Liang, L.; McCarthy, J. F.
734 Adsorption and desorption of natural organic matter on iron oxide:
735 mechanisms and models. *Environ. Sci. Technol.* **1994**, *28* (1), 38–46.

736 (43) Gu, B.; Schmitt, J.; Chen, Z.; Liang, L.; McCarthy, J. F.
737 Adsorption and desorption of different organic matter fractions on
738 iron oxide. *Geochim. Cosmochim. Acta* **1995**, *59* (2), 219–229.

739 (44) Miller, C. L.; Liang, L.; Gu, B. Competitive ligand exchange
740 reveals time dependant changes in the reactivity of Hg–dissolved
741 organic matter complexes. *Environ. Chem.* **2012**, *9* (6), 495–501.

742 (45) Vieira, A. P.; Berndt, G.; de Souza Junior, I. G.; Di Mauro, E.;
743 Paesano, A.; de Santana, H.; da Costa, A. C. S.; Zaia, C. T. B. V.; Zaia,
744 D. A. M. Adsorption of cysteine on hematite, magnetite and
745 ferrihydrite: FT-IR, Mössbauer, EPR spectroscopy and X-ray
746 diffractometry studies. *Amino Acids* **2011**, *40* (1), 205–214.

747 (46) Schwaminger, S. P.; García, P. F.; Merck, G. K.; Bodensteiner,
748 F. A.; Heissler, S.; Günther, S.; Berensmeier, S. Nature of Interactions
749 of Amino Acids with Bare Magnetite Nanoparticles. *J. Phys. Chem. C*
750 **2015**, *119* (40), 23032–23041.

751 (47) Donovan, P. M.; Blum, J. D.; Demers, J. D.; Gu, B.; Brooks, S.
752 C.; Peryam, J. Identification of Multiple Mercury Sources to Stream
753 Sediments near Oak Ridge, TN, USA. *Environ. Sci. Technol.* **2014**, *48*
754 (7), 3666–3674.

755 (48) Herrero, R.; Lodeiro, P.; Rey-Castro, C.; Vilariño, T.; De
756 Vicente, M. E. S. Removal of inorganic mercury from aqueous
757 solutions by biomass of the marine macroalga *Cystoseira baccata*.
758 *Water Res.* **2005**, *39* (14), 3199–3210.

759 (49) Green-Ruiz, C. Mercury (II) removal from aqueous solutions
760 by nonviable *Bacillus* sp. from a tropical estuary. *Bioresour. Technol.*
761 **2006**, *97* (15), 1907–1911.

762 (50) Zaferani, S.; Pérez-Rodríguez, M.; Biester, H. Diatom ooze—A
763 large marine mercury sink. *Science* **2018**, *361* (6404), 797–800.

764 (51) Gu, B.; Bian, Y.; Miller, C. L.; Dong, W.; Jiang, X.; Liang, L.
765 Mercury reduction and complexation by natural organic matter in
766 anoxic environments. *Proc. Natl. Acad. Sci. U. S. A.* **2011**, *108* (4),
767 1479–1483.

768 (52) George, G. N.; Prince, R. C.; Gailer, J.; Buttigieg, G. A.;
769 Denton, M. B.; Harris, H. H.; Pickering, I. J. Mercury binding to the
770 chelation therapy agents DMSA and DMPS and the rational design of
771 custom chelators for mercury. *Chem. Res. Toxicol.* **2004**, *17* (8), 999–
772 1006.

773 (53) Collins, C. R.; Sherman, D. M.; Ragnarsdóttir, K. V. Surface
774 Complexation of Hg^{2+} on Goethite: Mechanism from EXAFS
775 Spectroscopy and Density Functional Calculations. *J. Colloid Interface
776 Sci.* **1999**, *219* (2), 345–350.

777 (54) Brigatti, M.; Colonna, S.; Malferrari, D.; Medici, L.; Poppi, L.
778 Mercury adsorption by montmorillonite and vermiculite: a combined
779 XRD, TG-MS, and EXAFS study. *Appl. Clay Sci.* **2005**, *28* (1–4), 1–
780 8.

781 (55) Jiskra, M.; Saile, D.; Wiederhold, J. G.; Bourdon, B.; Björn, E.;
782 Kretzschmar, R. Kinetics of Hg(II) Exchange between Organic
783 Ligands, Goethite, and Natural Organic Matter Studied with an
784 Enriched Stable Isotope Approach. *Environ. Sci. Technol.* **2014**, *48*
785 (22), 13207–13217.

786 (56) Barrow, N.; Brümmer, G.; Fischer, L. Rate of desorption of
787 eight heavy metals from goethite and its implications for under-
788 standing the pathways for penetration. *Eur. J. Soil Sci.* **2012**, *63* (3),
789 389–398.

790 (57) Jiang, P.; Li, Y.; Liu, G.; Yang, G.; Lagos, L.; Yin, Y.; Gu, B.;
791 Jiang, G.; Cai, Y. Evaluating the role of re-adsorption of dissolved
792 Hg^{2+} during cinnabar dissolution using isotope tracer technique. *J.
793 Hazard. Mater.* **2016**, *317*, 466–475.

794 (58) Poulin, B. A.; Gerbig, C. A.; Kim, C. S.; Stegemeier, J. P.; Ryan,
795 J. N.; Aiken, G. R. Effects of Sulfide Concentration and Dissolved
796 Organic Matter Characteristics on the Structure of Nanocolloidal 796
797 Metacinnabar. *Environ. Sci. Technol.* **2017**, *51* (22), 13133–13142.

798 (59) Ravichandran, M.; Aiken, G. R.; Reddy, M. M.; Ryan, J. N. 799
Enhanced dissolution of cinnabar (mercuric sulfide) by dissolved 799
organic matter isolated from the Florida Everglades. *Environ. Sci. 800
Technol.* **1998**, *32* (21), 3305–3311.

801 (60) Yang, Z.; Fang, W.; Lu, X.; Sheng, G.-P.; Graham, D. E.; Liang,
802 L.; Wullschleger, S. D.; Gu, B. Warming increases methylmercury 803
production in an Arctic soil. *Environ. Pollut.* **2016**, *214*, 504–509.

804 (61) Olsen, T. A.; Muller, K. A.; Painter, S. L.; Brooks, S. C. Kinetics 805
of Methylmercury Production Revisited. *Environ. Sci. Technol.* **2018**, *52* (4),
806 2063–2070.

807 (62) Wang, Y.; Schaefer, J. K.; Mishra, B.; Yee, N. Intracellular Hg 808
808 (0) Oxidation in Desulfovibrio desulfuricans ND132. *Environ. Sci. 809
Technol.* **2016**, *50* (20), 11049–11056.

810 (63) Lin, H.; Morrell-Falvey, J. L.; Rao, B.; Liang, L.; Gu, B. 811
Coupled Mercury–Cell Sorption, Reduction, and Oxidation on 812
812 Methylmercury Production by *Geobacter sulfurreducens* PCA. *813
Environ. Sci. Technol.* **2014**, *48* (20), 11969–11976.

814 (64) Foucher, D.; Hintelmann, H. Tracing mercury contamination 815
from the Idrija mining region (Slovenia) to the Gulf of Trieste using 816
816 Hg isotope ratio measurements. *Environ. Sci. Technol.* **2009**, *43* (1),
817 33–39.

818 (65) Mason, R. P.; Choi, A. L.; Fitzgerald, W. F.; Hammerschmidt,
819 C. R.; Lamborg, C. H.; Soerensen, A. L.; Sunderland, E. M. Mercury 820
820 biogeochemical cycling in the ocean and policy implications. *Environ. 821
Res.* **2012**, *119*, 101–117.

822 (66) Driscoll, C. T.; Mason, R. P.; Chan, H. M.; Jacob, D. J.;
823 Pirrone, N. Mercury as a global pollutant: sources, pathways, and 824
824 effects. *Environ. Sci. Technol.* **2013**, *47* (10), 4967–4983.

825 (67) Fitzgerald, W. F.; Lamborg, C. H.; Hammerschmidt, C. R. 826
Marine biogeochemical cycling of mercury. *Chem. Rev.* **2007**, *107* (2),
827 641–662.

828 (68) Bouchet, S.; Goñi-Urriza, M.; Monperrus, M.; Guyoneaud, R.;
829 Fernandez, P.; Heredia, C.; Tessier, E.; Gassie, C.; Point, D.;
830 Guédron, S. Linking microbial activities and low molecular weight 831
831 thiols to Hg methylation in biofilms and periphyton from high 832
832 altitude tropical lakes (Bolivian altiplano). *Environ. Sci. Technol.* **2018**, *833*
833 (52), 9758–9767.

834 (69) Olsen, T. A.; Brandt, C. C.; Brooks, S. C. Periphyton biofilms 835
835 influence net methylmercury production in an industrially contami- 836
nated system. *Environ. Sci. Technol.* **2016**, *50* (20), 10843–10850.

837